Selection of RNA amide synthases

Torsten W Wiegand, Rachel C Janssen and Bruce E Eaton

Background: It is generally accepted that, during evolution, replicating RNA molecules emerged from pools of random polynucleotides. This prebiotic RNA world was followed by an era of RNA-mediated catalysis of amide-bond formation. RNA would thus have provided the machinery responsible for the assembly of peptides and the beginning of the protein world of today. Naturally occurring ribozymes, which catalyze the cleavage or ligation of oligonucleotide phosphodiester bonds, support the idea that RNA could self-replicate. But was RNA constrained to this path and were RNA-acylated carriers required before RNA could catalyze the formation of amide bonds?

Results: We have isolated RNA catalysts that are capable of mediating amide-bond synthesis without the need for specifically designed templates to align the substrates, and we have kinetically characterized these catalysts. The rate enhancement observed for these RNA amide synthases exceeds the noncatalyzed amidation rate by a factor of ~10^4. In addition, Cu^{2+} ions caused a change in the affinity of RNA for the substrate rather than being directly involved in amide-bond formation.

Conclusions: The discovery of these new amide synthases shows how functionally modified nucleic acids can facilitate covalent-bond formation without templating. Previously unforeseen RNA-evolution pathways can, therefore, be considered; for example, to guide amide-bond formation, *en route* to the protein world, it appears that substrate-binding pockets were formed that are analogous to those of protein enzymes.

Address: NeXstar Pharmaceuticals Incorporated, 2860 Wilderness Place, Boulder, CO 80301, USA.

Correspondence: Bruce E Eaton
E-mail: beaton@nexstar.com

Key words: amide synthase, catalytic RNA, copper metalloenzyme, *in vitro* selection, RNA world

Received: **11 July 1997**
Revisions requested: **28 July 1997**
Revisions received: **7 August 1997**
Accepted: **8 August 1997**

Chemistry & Biology September 1997, **4**:675–683
http://biomednet.com/elecref/1074552100400675

Introduction

Research on RNA catalyzed reactions has implications for the origin of life on earth. It is generally accepted that self-replicating RNA molecules emerged from pools of random polynucleotides to establish a prebiotic RNA world, which was followed by the historic moment when RNA molecules catalyzed the formation of the first amide bonds, rendering the protein world possible [1–3]. The underlying assumption of this hypothesis has been that an evolving population of self-replicating RNA molecules must have formed the machinery, including acylated adaptor molecules, responsible for the assembly of peptides as known in contemporary biochemistry.

The discovery of naturally occurring ribozymes (for nomenclature, see the Materials and methods section) [4–8], all of which catalyze the cleavage or ligation of oligonucleotide phosphodiester bonds, supports the notion that RNA could replicate itself. But the questions arise of whether or not the RNA world was constrained to this evolutionary path and whether it was necessary for RNA-acylated carriers to be prepared before RNA could catalyze the formation of amide bonds. Here, we describe families of RNA amide synthases that do not require any of the templating reminiscent of the biosynthetic schemes common to the protein world of today. Unshackled from this requirement for templating, RNA may have been free to catalyze the synthesis of not just peptides but also other cofactors required for the transition from the RNA to the protein world.

The first report of an RNA-catalyzed reaction (5–15-fold rate enhancement) at a carbon center involved the hydrolysis of an aminoacyl ester by the *Tetrahymena* ribozyme [9]. Since then, RNA catalysis has been expanded by *in vitro* selection techniques to include reactions in which one small molecule reacts on the RNA [10–14]. Preselection of substrate-binding sites in the catalysts or selection via transition-state analogs have proven to be successful [15–17], but only one example of an RNA amide synthase has been reported previously [18]. In this elegant work a six-residue RNA substrate (6-mer) was used to template a 3′-*N*-biotinmethionine-ester in proximity to a 5′-amino modified RNA so that juxtaposition of the two RNA molecules by nucleic acid hybridization afforded amide-bond formation. This demonstrated the ability of an RNA-acylated donor to form amide bonds with the aid of a suitable folded RNA and so affect catalysis, mimicking the functions of the ribosomal and transfer RNAs, well known in protein biosynthesis.

In vitro selection (SELEX) [19–22] has been used to show that RNA can exhibit exquisite molecular recognition in binding a broad array of small molecules, including amino

Figure 1

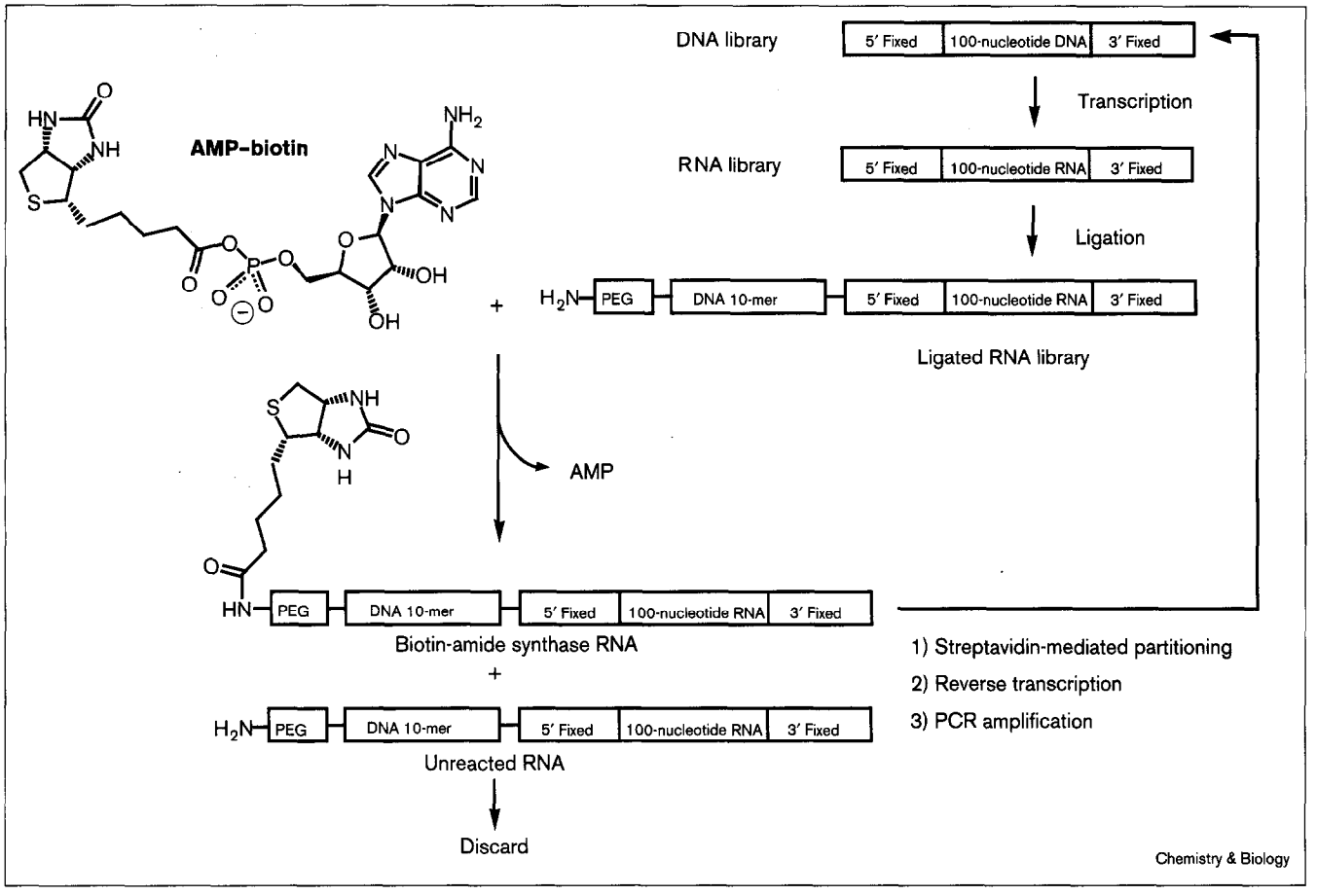

The procedure for the isolation of RNA amide synthases. Catalytic RNA molecules in the modified ligated RNA library catalyze the formation of an amide bond between a primary amine at the terminus of a polyethylene glycol (PEG) linker and the carboxyl group of AMP–biotin. The resulting biotin-amide is used for partitioning during *in vitro* selection rounds and during kinetic analysis of isolated RNA amide synthases. PCR, polymerase chain reaction.

acids [23–26], xanthines [27] and aminoglycosides [28–30]. But RNA libraries and selection strategies have yet to be described that would bring two small-molecule substrates together to yield an equally broad spectrum of RNA catalysis in which nucleic acid hybridization of substrates is not required. Here, we describe the isolation and kinetic characterization of amide synthase RNA molecules that catalyze the reaction of an amide bond between a simple primary amine and the carboxy carbonyl of AMP–biotin without the involvement of a template to align the substrates.

Results and discussion

Selection of amide synthases

The selection procedure for the isolation of RNA amide synthases is outlined in Figure 1. Transcriptions were carried out in the presence of ATP, CTP, GTP and 5-imidazole-UTP instead of UTP [31]. Experience in selection of RNA catalysts for related carbonyl reactions has shown that significantly reduced rate enhancements are observed without such modification of UTP (D.A. Nieuwlandt, M.C. West., G. Kirschenheuter, X. Cheng and B.E.E., unpublished observations). The importance of modified nucleotide bases in RNA evolution has been discussed previously [32,33]. Inclusion of the modified UTP was envisaged to enhance the catalytic power of RNA in general acid/base catalysis, as well as providing metal-coordination sites that could play a role in either catalysis or structure. A simple primary amine was connected by a long polyethylene glycol (PEG) linker so that it would simulate a free amine in solution. This amine substrate was located at the end of a 2 kDa PEG linker that was attached to the RNA library through a 10-nucleotide single-stranded DNA segment by bridged ligation. PEG was chosen as the linker because it is well solvated, flexible, and has no significant affinity for oligonucleotides, while it maintains the covalent linkage required for co-isolation of the product and the corresponding catalytic RNA. The length of this linker is intended to allow the amine substrate free access to any portion of the folded RNA structure.

Figure 2

(a)

AS23 3
gggagacaagaauaaacgcucaaUCCCAGUCC GGUAAUAAGGAUG GAGUCCUCGGACGGGGCCAGGUAGUGAGCCGUAAUGGCUGAAAGGUUGUGAUACGGGUUGUUUUGACGCGUAAGCGGCuucgacaggaggcucacaacaggc
AS30 1
gggagacaagaauaaacgnucaaGAUCGACCUCCGUACCUGCGGGUUC GGUAAUUGGGAUG AACGAAAUCCCAUGAACCCAGCUUUGUGUGACCUCCGAGCCUAGGGGAAAGGAUUCACUCAuucgacaggaggcucacaacaggc
AS05 16
gggagacaagaauaaacgcucaaUCGCCAGCGUGCAAUCAAUUGCGCGUAGCG GGUAAUAAGGAUU GUGCGUGGGGAGCCCAACGUGACUGGCACUGGAAGAGCACGGGCGUCUCUAAGCGuucgacaggaggcucacaacaggc
AS40 1
gggagacaagaauaaacguucaaGGUCACCUGUUGUAGAAACGGAACACCGCUCACAGUACCG CGUAAUAAGGAUU AGACCCAUGAGCUAGCGUGCCAUCCUAAGGUACUGGCUGGAGCCuucgacaggaggcuucacaacaggc
AS08 7
gggagacaagaauaaacgcucaaGUGGCUGGAGCACGCCAGCACUUGCGUUAGCUGUGGCACCCGGCCUUG GGUAAUUGGGAUG AGAUCCUAUGGGUUCCGGGGCGCAGUAUGUAAAUGCCuucgacaggaggcucacaacaggc
AS42 1
gggagacaagaauaaacgcucaaCGGAGCGUAAUCGUGGUAAGUGCUGAGACACUUGGCACGAAGCGGUAUUC UGUAAUCGGGAUG GUUCCGGUCUUGUAAGGCUGUUAGGGCUGGGGCuucgacaggaggcuacacaacaggc
AS02 5
gggagacaagaauaaacgcucaaUACCAGCGGGGCAGCCGCGGGGAAACACCAGUGAGGGAUGUGCGCGACGGCGCCG GGUAAUUGGGAUU GAGCGGUGUUCGUGAUCGGGGACCUGCGAACCuucgacaggaggcucacaacaggc
AS20 1
gggagacaagaauaaacgcucaaAUCCUGGCGCCCGGAAGCCUGGGAUGUACGCGUCUGAGGGCGGCCAUGUCAGGGGCGA CGUAAUCUGGAUU UGCAGGCGUGAUCUUAGGUGGUUGGGUGCuucgacaggaggcucacaacaggc
AS09 3
gggagacaagaauaaacgcucaaUACCAAGCGGGUUUGAGGGUAGGCUCGAGGGGAAACUCCAGCCGGUCACUAAUCCACGCU GGUAAUUGGGAUU GAGCGUUGUCUGCCGGGCAGAGGUGCuucgacaggaggcucacaacaggc
AS01 2
gggagacaaggaauaaacgcucaaGCAUGGGUACGGGCGCGGACGGACGUGCUGUACCAGUCUUGCGCGUUAAUGAUCGCGCGUGCG CGUAAUAUGGAUG AUUCCUUAGCCGUAGUGUGUuucgacaggaggcucacaacaggc
AS04 2
gggagacaagaauaaacgcucaaGCAAUCAGUGGUAUAAAGACCGUCCACACAGACGGAUAGGCUGUUCAUUCUGAAUGCUGACCGGAACG UUUAAUCAGGAUC AAACAUCCUACGUUCGuucgacaggaggcucacaacaggc
AS07 1
gggagacaagaauaaacgcucaaACAGACGGAACGUCGGCGGCGCCACACACUGUCGAGAGCAAAGGUAUUCCAUGUCUAGACCGCGAUAUUGGUCACCC UGUAAUAAGGACG CGAUCCUAGGuucgacaggaggcucacaacaggc
AS25 2
gggagacaagaauaaacgcucaaAGGCUAUAAGCUGAGUUGCGUGUAUUGCUGUGACCGCGAUCCCCGGCGGCUGCUUUCAGUCGAACUGCGUCUGCCGU GGUAAUCGGGAUG CUUGGUGCuucgacaggaggcucacaacaggc

AS03 1
gggagacaagaauaaacgcucaaCGCGUUAGUUCUGGGCCCGAUUAAACCAAACGGCCGCCGUUCAGGACUGCAUGCCAUUGUAUUGUUUGGGGAAGGGGUGGCGGCAACCACGCGCUGUGCCuucgacaggaggcucacaacaggc
AS26 1
gggagacaagaauaaacgcucaaUUUCAAGGCAGUGGCUGUGAUGGUUGAGAUUGAGGCGCUUUGGGGCCUGCACCGAUUUCAGGUGUGUAAGCAAGUUGUAUGAGUGUGGAGAACUGGCAuucgacaggaggcucacaacaggc
AS46 1
gggagacaagaauaaacgcucaaUAGCAGUCAGCAUGCACGCAGGCACCAAACAGUAGGGCUUGAGGGUUAGCGUCUAUCGUUGACGGGUGCGGUCUUGGCGUGUGGGGACGAGCUACGuucgacagaggcucacaacaggc

(b)

Position	1	2	3	4	5	6	7	8	9	10	11	12	13
A	0	0	0	**13**	**13**	0	**5**	**5**	0	0	**13**	0	0
C	**3**	0	0	0	0	0	**4**	0	0	0	0	1	1
G	**7**	**12**	0	0	0	0	0	**6**	**13**	**13**	0	0	**7**
U	**3**	1	**13**	0	0	**13**	**4**	2	0	0	0	**12**	**5**
Consensus	B	G	U	A	A	U	H	R	G	G	A	U	K

Chemistry & Biology

Amide synthase RNA sequences. **(a)** The upper 13 isolates form the amide synthase family containing a 13-nucleotide conserved sequence motif (boxed nucleotides). The lower three 'orphan' isolates show no apparent sequence homology to this family or to each other. Nucleotides forming the fixed regions (see Figure 1) are shown in lower case letters. The numbers after the sequence designation indicate the frequency with which an isolate was found by sequence analysis. **(b)** Occurrences of individual nucleotides at each position of the sequence motif are listed. Abbreviations for variant positions: R, A or G; Y, C or U; K, G or U; H, A or C or U; B, C or G or U.

RNA libraries were incubated with AMP–biotin at 25°C, pH 7, in a buffer containing monovalent and divalent metal ions including first-row transition metals that could form Lewis acid sites on coordination to the RNA [34,35]. Amide synthase RNA catalysts were partitioned based on the formation of biotin amide, by streptavidin-induced gel retardation or by immobilization on streptavidin-coated magnetic beads. After reverse transcription, polymerase chain reaction (PCR) amplification of the DNA template, and transcription, the RNA was re-ligated to DNA–PEG-NH_2 to prepare the enriched library for the subsequent round. The stringency of the reaction conditions was gradually increased over the course of the selection by decreasing the AMP–biotin concentration from 10 mM to 20 μM, the RNA concentration from 10 μM to 0.1 μM and by shortening the incubation time from 16 h to 10 min. By round 16, the extent of RNA catalyzed amidation had reached a maximum. Amide synthase activity of the selected RNA library was shown to be dependent on the presence of AMP–biotin and the PEG-linked amine.

Cloning and sequencing of 48 members of this library led to the identification of 16 distinct sequences, 13 of which can be grouped into a family based on a common 13-nucleotide conserved motif (Figure 2). The remaining three sequences, so called 'orphans', do not share any primary sequence homology with this family or with each other. Based on a thermodynamic folding algorithm [36], the sequences of the amide synthase family are predicted to contain a secondary structure core (Figure 3a) of which the 13-nucleotide sequence motif is an integral part. This core structure consists of a 3–9 base-pair stem with little or no primary sequence conservation, followed by a 5–10 nucleotide bulge, presenting the invariant 5′-UAAU-3′

Figure 3

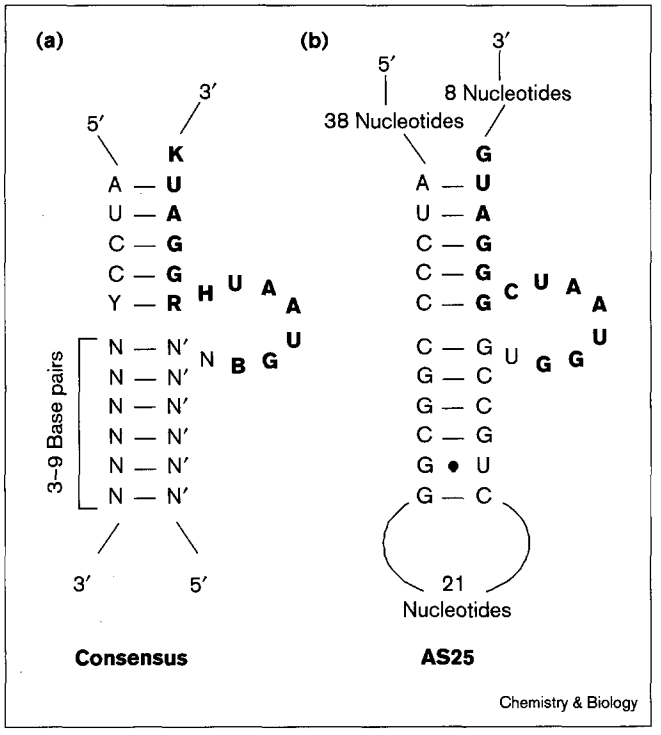

The proposed secondary structure of the amide synthase RNA sequence core. **(a)** This conserved stem–bulge–stem structure is found in all of the isolates comprising the amide synthase RNA family. Although the top stem is very sequence specific, the bottom stem appears to require little or no primary sequence conservation. The ends of the RNA molecules can be located at either end of the structural core, resulting in circular permutations. **(b)** The structural core of AS25, the most studied amide synthase, is shown as an example. The 13-nucleotide conserved sequence is indicated in bold type. N, any nucleotide; N′, base-pairing nucleotide. The remaining nucleotide abbreviations are as described in Figure 2. Non-Watson–Crick base pairing is indicated by a connecting dot instead of a line.

Figure 4

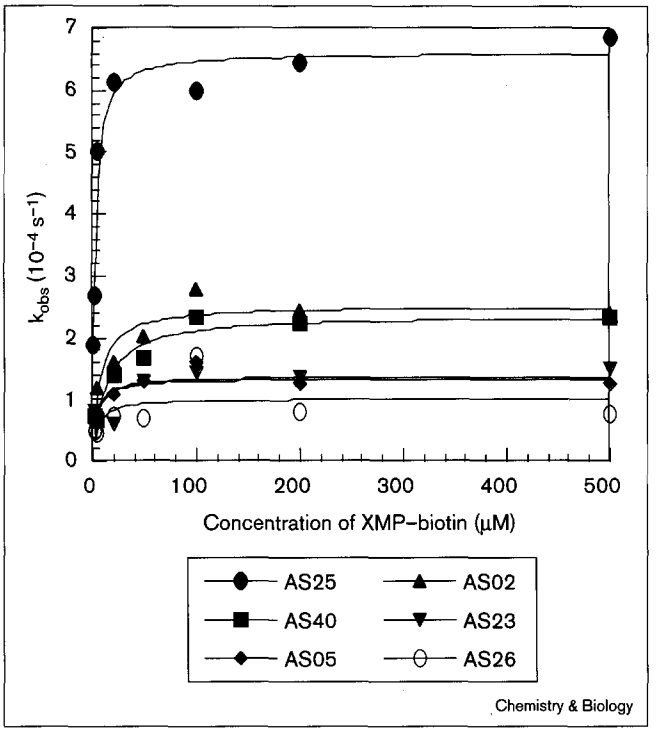

Determination of K_m (achieved by non-linear least square regression data) and k_{cat} (Michaelis–Menton first-order rate constant for catalysis) values for RNA amide synthases. RNA–DNA–PEG-NH_2 molecules (0.1 μM) were incubated with nucleoside-monophosphate–biotin substrates in reaction buffer (see Materials and methods section) at 25°C. Reactions were quenched by addition of excess streptavidin and the fraction of RNA biotin-amide formation was determined by mobility shift assays on denaturing polyacrylamide gels. By following the fraction of RNA biotin-amide formation over time, k_{obs} (observed first-order rate constant) values were obtained for each substrate concentration. Values for K_m and k_{cat} were determined by plotting k_{obs} versus substrate concentration and are summarized in Table 1. AS26 is an orphan sequence, the other five isolates are members of the amide synthase family. For comparison, the data for AS25 are also shown in Figures 5b and 6.

sequence core, and a 5 base-pair stem with high sequence conservation. Although 5′–3′ directionality within this structural motif is conserved among the sequence families, the location within the RNA varies, resulting in circular permutations of the sequence.

As a representative example of a specific family member, the predicted secondary structure of the most studied amide synthase, isolate AS25 (see below), is shown in Figure 3b. The folding algorithm ignores the contributions of the modified uridines, but it is apparent, based on sequence conservation, that the RNA core containing three 5-imidazole-uridine nucleotides is required for amide synthase activity. To test whether the imidazole groups were essential for catalysis, the AS25 sequence was transcribed using native UTP. This RNA showed no amide synthase activity, consistent with the modified uridine playing an important role in catalysis. The structural or catalytic role of the imidazole modification in these amide synthases remains to be understood.

Amide synthase rate enhancement

To survey the catalytic activity of the amide synthases, K_m (substrate concentration at which half-maximal reaction rate is achieved) and k_{cat} (first-order rate constant for catalysis) values were determined for representative isolates (Figure 4 and Table 1). RNA amide synthases were incubated with various concentrations of AMP–biotin and the fraction of biotin-amide product was quantitated by gel electrophoretic mobility assays. These experiments were performed in a minimal reaction buffer (see Materials and methods section), containing only metal ions that are required for full amide synthase activity (see below). For all tested amide synthases the data were found to fit the standard Michaelis–Menten rate expression for a single turnover reaction at a single saturable substrate-binding site. Isolate AS25 was the most active catalyst, with both the lowest K_m value (2.3 μM) and the highest k_{cat} value

Table 1

A summary of the K_m and k_{cat} values for RNA amide synthases.

Isolate	Substrate	Cu^{2+} (10^{-6} M)	K_m	k_{cat} (10^{-4} s^{-1})	Rate enhancement (10^4)
AS25	AMP–biotin	+	2.3 ± 0.4	6.6 ± 0.2	11.0
	AMP–biotin	–	23.6 ± 10.1	6.9 ± 0.6	
	UMP–biotin	+	1.4 ± 0.3	6.8 ± 0.3	
	RMP–biotin	+	1.9 ± 0.9	6.2 ± 0.5	
AS40	AMP–biotin	+	12.2 ± 4.2	2.4 ± 0.2	0.7
AS05	AMP–biotin	+	4.0 ± 1.7	1.4 ± 0.1	1.3
AS02	AMP–biotin	+	6.6 ± 2.3	2.5 ± 0.2	1.5
AS23	AMP–biotin	+	3.9 ± 2.9	1.3 ± 0.2	1.4
AS26	AMP–biotin	+	4.3 ± 5.3	1.0 ± 0.2	0.9

The determinations of K_m and k_{cat} values are described in Figure 4.

(6.6×10^{-4} s^{-1}) of the RNA amide synthases. The remaining isolates of this sequence family have higher K_m and lower k_{cat} values. This could be attributed to minor variations in the 13-nucleotide consensus region, but it is probable that amide synthase activity may also be affected by other regions of the RNA. Kinetic values for the orphan sequence AS26 suggest that it is essentially an equivalent amide synthase to the unrelated sequence family of which AS25 is a member. It appears that from these modified RNA libraries multiple catalytic motifs can be isolated.

To calculate the rate enhancement achieved by amide synthase AS25, the spontaneous background reaction was estimated. Obtaining measurable product formation for these spontaneous amidation reactions requires the use of higher substrate concentrations and longer reaction times. Under these conditions amidation occurs at both the terminal amine and at internal nucleophilic atoms, presumably exo-cyclic amines on the nucleotide bases. The apparent background second-order rate constant was, therefore, determined for a randomized RNA–DNA–PEG-NH_2 library (3.8×10^{-3} s^{-1} M^{-1}) and an equivalent library in which the amine was replaced by an unreactive methylether group (1.2×10^{-3} s^{-1} M^{-1}). The difference, 2.6×10^{-3} s^{-1} M^{-1}, gives an estimate of the non-facilitated second-order rate constant for amidation of the terminal amine. Caution must be exercised, however, when viewing these background rate determinations, because only initial rates can be measured. The rate enhancement (RE) for AS25 was calculated as follows:

$$RE_{AS25} = \left(\frac{k_{cat}}{K_m}\right)\left(\frac{1}{k_{uncat}}\right) = \left(\frac{6.6\times10^{-4}\,s^{-1}}{2.3\times10^{-6}\,M}\right)\left(\frac{1}{2.6\times10^{3}\,s^{-1}M^{-1}}\right) = 1.1\times10^{5} \quad (1)$$

The RE observed for AS25 is larger than 10^5, clearly more than sufficient to support the notion of RNA evolution of non-templated amide bond formation. Compared to AS25, the remaining amide synthases are only slightly less efficient with rate enhancements of ~10^4 (Table 1).

Amide synthase metal dependence

The fastest amide synthase, isolate AS25, was chosen for a more detailed analysis of reaction condition requirements. ^{32}P-labeled AS25–DNA–PEG-NH_2 was incubated with AMP–biotin in the standard reaction buffer and variations thereof that differ in divalent-cation composition. Figure 5a shows the fraction of AS25 amidation over 1 h under these conditions. The slowest reaction rate was observed in the absence of divalent metal ions (open circles), but this rate is still significantly faster than the spontaneous background reaction. The RNA amide synthase rate was increased by addition of divalent cations (open diamonds) with Ca^{2+} (open squares) being slightly more effective than Mg^{2+} (open triangles). Addition of each of the individual transition-metal ions and a systematic analysis of combinations (data not shown) demonstrated that Cu^{2+} (closed symbols) significantly increases the rate of AS25 catalyzed amidation. The other five transition metals (Co^{2+}, Fe^{2+}, Mn^{2+}, Ni^{2+}, and Zn^{2+}) have no effect on catalysis. Values for K_m and k_{cat} were determined for amide synthase AS25 in the presence and absence of Cu^{2+} (10 μM) (Figure 5b). Interestingly, k_{cat} was unchanged, but K_m was increased from 2.3 μM to 23.6 μM in the absence of Cu^{2+}. These results suggest that Cu^{2+} ions cause a change in the affinity of the RNA for the substrate, rather than being directly involved in the amide-bond-forming step.

Identification of the amide product

The tethered amine was required to observe amide synthase activity for all of the RNA catalysts. It needed to be

Figure 5

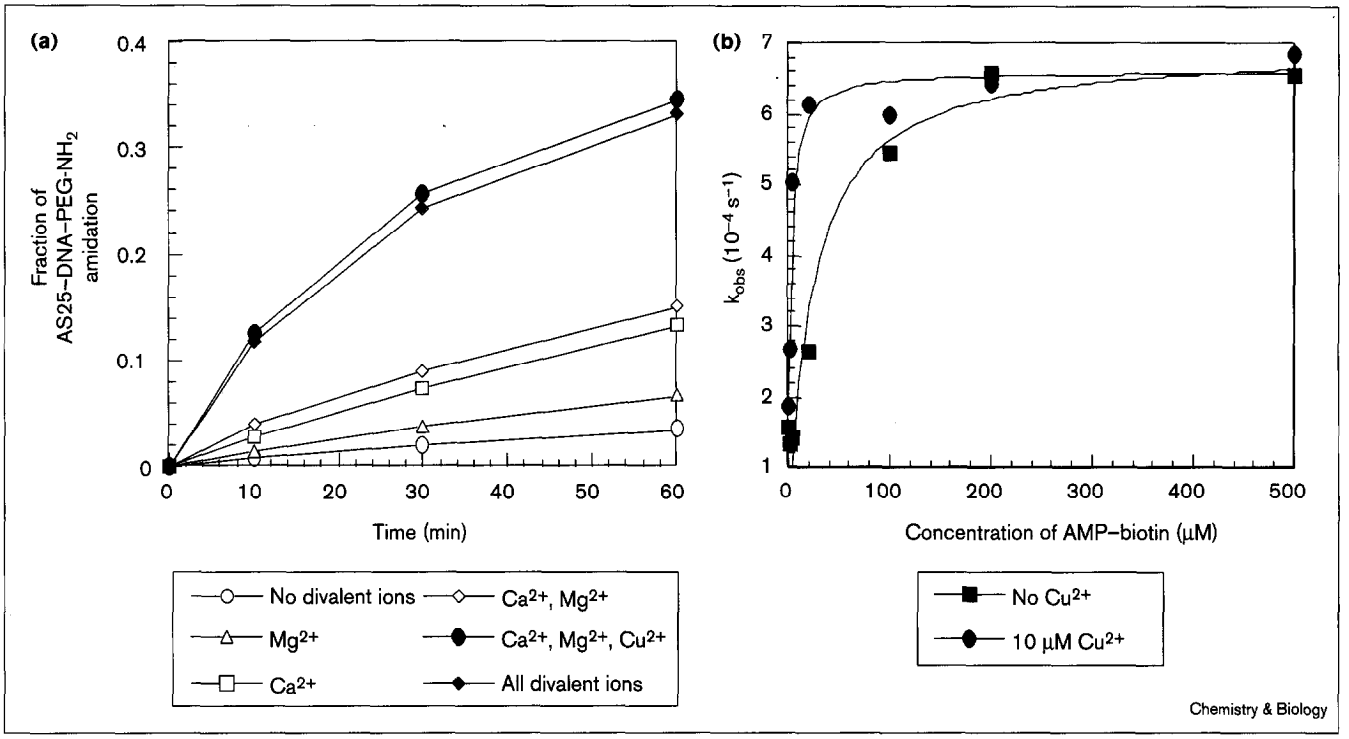

The metal dependence of amide synthase activity for isolate AS25. Amide synthase AS25 (0.1 μM) was incubated with AMP–biotin (20 μM) under various conditions. **(a)** The reaction buffer contained various combinations of divalent metal ions (100 mM HEPES pH 7, 200 mM NaCl, 200 mM KCl, ± 2 mM $MgCl_2$, ± 2 mM $CaCl_2$, ± 10 μM $CoCl_2$, ± 10 μM $CuCl_2$, ± 10 μM $FeCl_2$, ± 10 μM $MnCl_2$, ± 10 μM $NiCl_2$, and ± 10 μM $ZnCl_2$) at 25°C. Kinetic analysis was performed as described in Figure 4. Closed symbols represent reaction conditions that include Cu^{2+} ions while open symbols indicate the absence of Cu^{2+}. **(b)** The reaction buffer contained only $MgCl_2$ and $CaCl_2$ as sources for divalent metal ions (squares) or additionally 10 μM Cu^{2+} (circles). Values for K_m and k_{cat} are listed in Table 1.

proven, however, that AMP–biotin had not reacted with any of the >150 amino or hydroxyl groups present in the oligonucleotide portion of AS25. To reject the possibility of linkage anywhere on the RNA, the biotinylated AS25 reaction product was digested with ribonuclease I followed by complete chemical cleavage of the DNA. Electrospray mass spectrometry (ESMS) analysis of this digested sample gave a mass value consistent with a molecule containing the biotin-amide product and a single phosphate group (a remnant from the 5′-end of the DNA) separated by the PEG linker, thus demonstrating that the biotin had reacted to form an amide bond with the tethered amine.

Substrate recognition

It was important to determine if the AMP–biotin was serving as an RNA-acylated substrate, in effect templating the amidation reaction. To determine whether AMP was involved in substrate recognition by Watson–Crick base pairing to a residue in the RNA catalytic site, two alternative substrates were tested for reactivity with AS25–DNA–PEG-NH_2. UMP–biotin was used to test the effect of altering the hydrogen-bond donor and acceptor pattern. RMP–biotin (5-ribose-monophosphate–biotin) was used to determine whether any base pairing was required to observe catalytic activity. For these substrates, K_m and k_{cat} values of isolate AS25 (Figure 6) were virtually identical to those of AMP–biotin, demonstrating that both substrate recognition and amidation rates were unchanged. Amide synthase AS25 does not, therefore, appear to use the adenine base as a template to align the substrate.

Having ruled out an important role for the nucleotide base, individual contributions of the ribose-phosphate and biotin for substrate recognition remained to be tested. Kinetic inhibition experiments were performed with AMP and biotin. These potential competitors were added to reactions catalyzed by AS25–DNA–PEG-NH_2 under conditions where biotin-amide formation was linear with respect to time and AMP–biotin concentration. Product formation was plotted against inhibitor concentration as shown in Figure 7. A 500-fold molar excess (10 mM) of free AMP did not inhibit the amide synthase reaction. This is further evidence that the adenine portion of AMP–biotin is not important for binding of the substrate in AS25. Because of the solubility limit in the aqueous reaction buffer, biotin could only be tested up

Figure 6

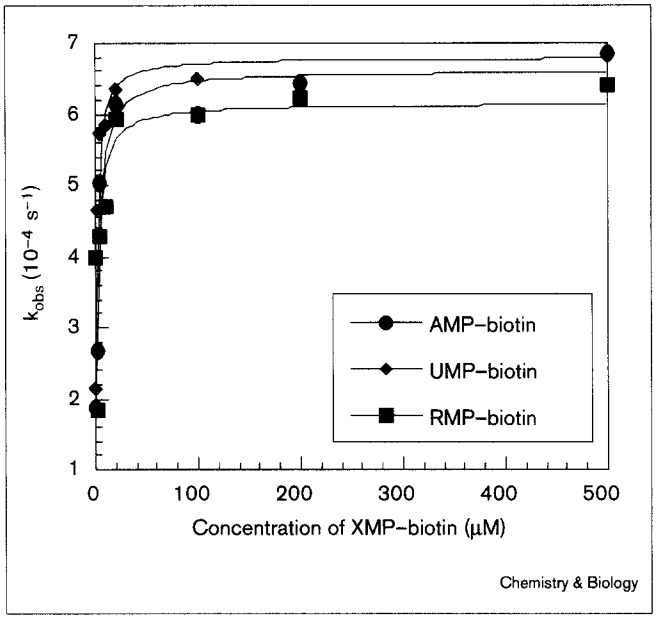

The effect of different substrates on amide synthase isolate AS25. Kinetic analysis was performed as described in Figure 4. UMP–biotin and RMP–biotin substrates were synthesized in an identical manner to AMP–biotin. Values for K_m and k_{cat} are listed in Table 1.

Figure 7

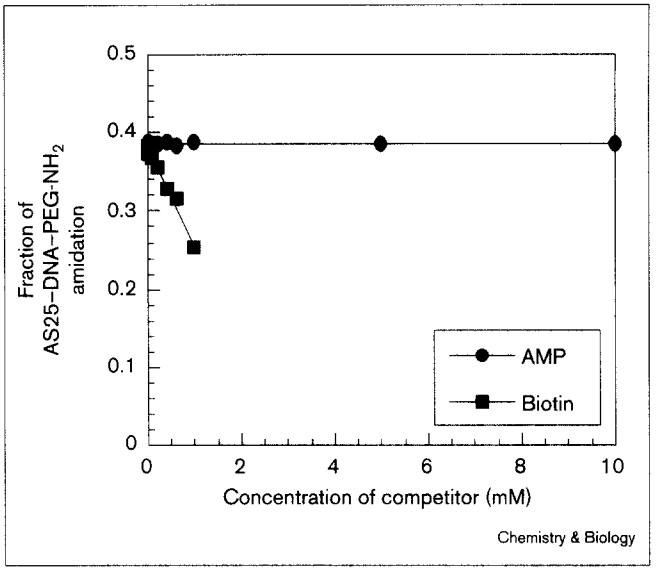

Inhibition of isolate AS25. AMP–biotin (20 mM) was mixed with various concentrations of AMP and biotin in minimal reaction buffer. Following addition of amide synthase AS25 (0.1 mM), the fraction of RNA biotin-amide formation was determined after 30 min. The inhibitory constant K_i for biotin is 240 mM, whereas AMP does not inhibit biotin-amide formation.

to a 50-fold molar excess (1 mM). In contrast to AMP, biotin inhibited the amide synthase reaction with a K_i (inhibitory constant) value of 240 μM and is, therefore, involved in substrate recognition.

Conclusions

The RNA amide synthases presented here catalyze the formation of an amide bond without predetermined substrate templating by Watson–Crick base-pairing. Instead, they appear to have formed substrate-binding pockets analogous to those of protein enzymes. Because RNA catalysis is now not limited to nucleic acid hybridization of substrates, new areas of chemistry may be explored, including chiral recognition of asymmetric substrates.

Significance

Self-replicating RNA molecules are thought to have evolved from pools of random polynucleotides, thereby establishing a prebiotic RNA world. This might then have been followed by the catalysis, by RNA molecules, of the formation of amide bonds, thus making possible the protein world of today.

Previously described ribozymes mediate phosphodiester-transfer reactions, but the discovery of RNA catalysts that are capable of enhancing amide-bond synthesis, without the need for specifically designed templates to align the substrates, makes plausible previously unforeseen RNA-evolution pathways.

Instead of requiring nucleic acids as templates to guide the amide-bond formation, these modified RNA catalysts appear to have formed substrate-binding pockets analogous to those of protein enzymes. With the realization that RNA catalysis is not limited to nucleic acid hybridization of substrates comes the potential to explore new dimensions of chemistry, including chiral recognition of asymmetric substrates.

The selection of catalysts by *in vitro* methodology allows for the incorporation of functional groups that have proven to be important for catalysis in organic synthesis. The properties of suitably modified catalytic RNA, as demonstrated by these amide synthases, make it feasible to test a combinatorial approach which could emulate evolution of the RNA world. In this *in vitro* world, RNA libraries and small-molecule product libraries may co-evolve, simulating the behavior of natural biological counterparts. These amide synthases therefore represent an important step in proving how universal RNA catalysis can be.

Materials and methods

Nomenclature

In accordance with the *Recommendations of the Commission on Biochemical Nomenclature on the Nomenclature and Classification of Enzymes* (1972), these catalytic RNA molecules have been designated as amide synthases to emphasize the synthetic aspect of the bond-formation reaction. Although the term ribozyme is useful to describe naturally occurring RNA molecules that catalyze phosphodiester-transfer

reactions, the expanding scope of RNA catalysts calls for the use of a more descriptive terminology in analogy to protein enzymes.

In vitro *selection*

The RNA library was created by transcription of PCR amplified DNA templates (40 mM Tris-HCl, pH 8.0; 4% PEG 8000; 12 mM $MgCl_2$; 5 mM dithiothreitol (DTT); 1 mM spermidine; 0.002% Triton X-100; 1 mM each of ATP, CTP, GTP, and 5-imidazole UTP; 20 mM GMP; 1.5 μM T7 RNA polymerase) to yield 5-imidazole uridine modified transcripts: 5′-GGGAGACAAGAAUAAACGCUCAA–100 nucleotides–UUCGACAGGAGGCUCACCACAGGC-3′. RNA molecules (10 μM) were ligated (70 mM Tris-HCl, pH 7.5; 12 mM KCl; 5 mM $MgCl_2$; 2 mM DTT; 1 mM ATP; 0.2 mM EDTA; 10% glycerol; 4 units/μl RNase inhibitor; 0.2 units/μl T4 DNA ligase, Boehringer Mannheim) to NH_2-PEG–5′-CCAGGCACGC-3′ substrate (20 μM) with the help of the bridging oligonucleotide (30 μM) 5′-CTTGTCTCCCGCGTGCCTGG-3′ at 37°C for 12 h. Ligated RNA molecules were purified by denaturing polyacrylamide gel electrophoresis and the RNA starting pool (2 nmol at 10 μM) was incubated with AMP–biotin (10 mM) in the reaction buffer (100 mM HEPES, pH 7; 200 mM NaCl; 200 mM KCl; 2 mM $MgCl_2$; 2 mM $CaCl_2$; 10 μM each of $CoCl_2$, $CuCl_2$, $FeCl_2$, $MnCl_2$, $NiCl_2$, and $ZnCl_2$) at 25°C for 16 h. Selection stringency was gradually increased by decreasing the RNA concentration to 0.1 μM, the AMP–biotin concentration to 20 μM, and the incubation time to 10 min. Reacted RNA molecules attached to the biotin-amide product were isolated by streptavidin-induced gel shift, in rounds 1–7 and round 11, or by binding to streptavidin coated magnetic beads (Dynabeads M-280; Dynal) in rounds 8–10 and rounds 12–20. Reverse transcription reactions of RNA molecules diffused from polyacrylamide gels, or attached to streptavidin beads were followed by PCR amplification to obtain DNA templates for the subsequent selection round.

Nucleoside-monophosphate–biotin preparation

To a mixture of 4.7 ml pyridine and 1.5 ml 0.5 N HCl, 1 mmol nucleoside-monophosphate (AMP, UMP, or RMP; Aldrich) and 1 mmol biotin (Sigma) were added. In 5 ml pyridine, 23 mmol 1,3-dicyclohexyl-carbodiimide (DCC) were dissolved and added to the AMP/biotin solution. The mixture was stirred at 20°C for 3 h and filtered to remove the side product 1,3-dicyclohexylurea (DCU). The filtrate was evaporated, resuspended in H_2O and purified by C18 high performance liquid chromatography (HPLC). To increase stability, 50 mg of NaCl were added to the AMP–biotin fraction before evaporation of the solvent. Since the nucleoside-monophosphate–biotin compounds slowly hydrolyze over time ($t_{1/2}$ ~4 days), preparations were re-quantitated before each use.

Kinetic analysis

Kinetic experiments were carried out at 0.1 μM RNA and nucleoside-monophosphate–biotin in the range 1–500 μM. With the exception of metal-dependence studies, all kinetic experiments were performed in the minimal reaction buffer containing 100 mM HEPES pH 7, 200 mM NaCl, 200 mM KCl, 2 mM $MgCl_2$, 2 mM $CaCl_2$, and 10 μM $CuCl_2$. Values for k_{obs} were obtained by fitting the fraction of unreacted RNA to the first-order reaction rate equation:

$$R = \alpha R_0 e^{(-k_{obs} t)} + (1 - \alpha R_0) \quad (2)$$

where R is the fraction of unreacted RNA, αR_0 is the functional fraction (α) of total RNA (R_0), t is time, and k_{obs} represents the first-order rate constant (k_{obs} is substrate concentration dependent and k_{cat} is not). The functional fraction of RNA was found to be 0.3–0.5, with the remaining RNA likely to be inactive due to alternative folding (data not shown). Values for k_{obs}, obtained for each substrate concentration, were entered into the Michaelis–Menten equation:

$$k_{obs} = \frac{k_{cat}[S]}{K_m + [S]} \quad (3)$$

where k_{cat} is the first-order rate constant, [S] is the substrate concentration, and K_m represents the substrate concentration at which half-maximal reaction rate is achieved. The inhibition constants K_i were determined after reacting 0.1 μM AS25–DNA–PEG-NH_2 with 20 μM AMP–biotin in the presence of 0–10 mM AMP or 0–1 mM biotin by fitting the fraction of biotinylated RNA to the following equation:

$$R_R = R_{R\,max} \left(\frac{S}{K_m}\right) \left(\frac{K_i + \frac{S}{K_m}}{1 + R_R}\right) \quad (4)$$

where R_R is the fraction of reacted RNA, $R_{R_{max}}$ is the maximum possible fraction of reacted RNA, S is the AMP–biotin concentration, K_m is the AMP–biotin concentration at half-maximal reaction rate, and K_i represents the inhibitory constant.

Product identification

2 nmol AS25–DNA–PEG-NH-biotin was digested with 400 units RNase I (Boehringer Mannheim) at 37°C for 1 h. The sample was purified and desalted by C4 HPLC and analyzed by ESMS. Degradation of the DNA was achieved by incubating ~200 pmol of the above described product in 240 μl 75% hydrazine at 20°C for 24 h. The sample was dried, resuspended in 500 μl piperidine, incubated at 90°C for 1 h, and dried again before ESMS analysis. Mass values were determined in negative ion mode for the −2 charge state and were within experimental error of the calculated masses.

Acknowledgements

We thank C. Zyzniewski and C. Tu for providing important compounds and D. Tinnermeier for performing mass spectrometry analysis. We are grateful to L. Wiegand, D. Smith, T. Tarasow, T. Dewey, D. Nieuwlandt, A. Pardi, E. Brody, and L. Gold for critical reading of the manuscript and many helpful discussions.

References

1. Joyce, G.F. (1996). Ribozymes: building the RNA world. *Curr. Biol.* **6**, 965-967.
2. Joyce, G.F. (1991). The rise and fall of the RNA world. *New Biol.* **3**, 399-407.
3. Bloch, K. (1996). Some biochemical thoughts on the RNA world. *Chem. Biol.* **3**, 405-407.
4. Cech, T.R. (1987). The chemistry of self-splicing RNA and RNA enzymes. *Science* **236**, 1532-1539.
5. Long, D.M. & Uhlenbeck, O.C. (1993). Self-cleaving catalytic RNA. *FASEB. J.* **7**, 25-30.
6. Bartel, D.P. & Szostak, J.W. (1993). Isolation of new ribozymes from a large pool of random sequences. *Science* **261**, 1411-1418.
7. Beaudry, A.A. & Joyce, G.F. (1992). Directed evolution of an RNA enzyme. *Science* **257**, 635-641.
8. Kumar, P.K.R. & Ellington, A.D. (1995). Artificial evolution and natural ribozymes. *FASEB. J.* **9**, 1183-1195.
9. Piccirilli, J.A., McConnell, T.S., Zaug, A.J., Noller, H.F. & Cech, T.R. (1992). Aminoacyl esterase activity of the *Tetrahymena* ribozyme. *Science* **256**, 1420-1424.
10. Lorsch, J.R. & Szostak, J.W. (1996). Chance and necessity in the selection of nucleic acid catalysts. *Acc. Chem. Res.* **29**, 103-110.
11. Wecker, M., Smith, D. & Gold, L. (1996). *In vitro* selection of a novel catalytic RNA: characterization of a sulfur alkylation reaction and interaction with a small peptide. *RNA* **2**, 982-994.
12. Illangasekare, M., Sanchez, G., Nickles, T. & Yarus, M. (1995). Aminoacyl-RNA synthesis catalyzed by an RNA. *Science* **267**, 643-647.
13. Wilson, C. & Szostak, J.W. (1995). *In vitro* evolution of a self-alkylating ribozyme. *Nature* **374**, 777-782.
14. Lorsch, J.R. & Szostak J.W. (1994). *In vitro* evolution of new ribozymes with polynucleotide kinase activity. *Nature* **371**, 31-36.
15. Conn, M.M., Prudent, J.R. & Schultz, P.G. (1996). Porphyrin metalation catalyzed by a small RNA molecule. *J. Am. Chem. Soc.* **118**, 7012-7013.
16. Li, Y. & Sen, D. (1996). A catalytic DNA for porphyrin metallation. *Nat. Struct. Biol.* **3**, 743-747.
17. Prudent, J.R., Uno, T. & Schultz, P.G. (1994). Expanding the scope of RNA catalysis. *Science* **264**, 1924-1927.
18. Lohse, P.A. & Szostak, J.W. (1996). Ribozyme-catalysed amino-acid transfer reactions. *Nature* **381**, 442-444.

19. Tuerk, C. & Gold, L. (1990). Systematic evolution of ligands by exponential enrichment: RNA ligands to bacteriophage T4 DNA polymerase. *Science* **249**, 505-510.
20. Ellington, A.D. & Szostak, J.W. (1990). *In vitro* selection of RNA molecules that bind specific ligands. *Nature* **346**, 818-822.
21. Gold, L., Polisky, B., Uhlenbeck, O. & Yarus, M. (1995). Diversity of oligonucleotide functions. *Annu. Rev. Biochem.* **64**, 763-797.
22. Gold, L. (1995). Oligonucleotides as research, diagnostic, and therapeutic agents. *J. Biol. Chem.* **270**, 13581-13584.
23. Famulok, M. (1994). Molecular recognition of amino acids by RNA-aptamers: an L-citrulline binding RNA motif and its evolution into an L-arginine binder. *J. Am. Chem. Soc.* **116**, 1698-1706.
24. Majerfeld, I. & Yarus, M. (1994). An RNA pocket for an aliphatic hydrophobe. *Nat. Struct. Biol.* **1**, 287-292.
25. Connell, G.J., Illangesekare, M. & Yarus, M. (1993). Three small ribooligonucleotides with specific arginine sites. *Biochemistry* **32**, 5497-5502.
26. Famulok, M. & Szostak, J.W. (1992). Stereospecific recognition of tryptophan agarose by *in vitro* selected RNA. *J. Am. Chem. Soc.* **114**, 3990-3991.
27. Jenison, R.D., Gill, S.C., Pardi, A. & Polisky, B. (1994). High-resolution molecular discrimination by RNA. *Science* **263**, 1425-1429.
28. Wang, Y., Killian, J., Hamasaki, K. & Rando, R.R. (1996). RNA molecules that specifically and stoichiometrically bind aminoglycoside antibiotics with high affinities. *Biochemistry* **35**, 12338-12346.
29. Lato, S.M., Boles, A.R. & Ellington, A.D. (1995). *In vitro* selection of RNA lectins: using combinatorial chemistry to interpret ribozyme evolution. *Chem. Biol.* **2**, 291-303.
30. Wallis, M.G., von Ahsen, U., Schroeder, R. & Famulok, M. (1995). A novel RNA motif for neomycin recognition. *Chem. Biol.* **2**, 543-552.
31. Dewey, T.M., Zyzniewski, M.C. & Eaton B.E. (1996). The RNA world: functional diversity in a nucleoside by carboxyamidation of uridine. *Nucl. Nucl.* **15**, 1611-1617.
32. Kolb, V.M., Dworkin, J.P. & Miller, S.L. (1994). Alternative bases in the RNA world: the prebiotic synthesis of urazole and its ribosides. *J. Mol. Evol.* **38**, 549-557.
33. Robertson, M.P. & Miller, S. (1995). Prebiotic synthesis of 5-substituted uracils: a bridge between the RNA world and the DNA-protein world. *Science* **268**, 702-705.
34. Kazakov, S.A. (1996). In *Biooganic Chemistry: Nucleic Acids* (Hecht, S.M., ed.), p. 244, New York.
35. Cotton, F.A. & Wilkinson, G. (1988). *Advanced Inorganic Chemistry* (5th edn), Wiley, New York.
36. Zuker, M. (1989). On finding all suboptimal foldings of an RNA molecule. *Science* **244**, 48-52.